

# Protease Activated Receptor-1 Deficiency Diminishes Bleomycin-Induced Skin Fibrosis

JanWillem Duitman,<sup>1</sup> Roberta R Ruela-de-Sousa,<sup>1</sup> Kun Shi,<sup>1</sup> Onno J de Boer,<sup>2</sup> Keren S Borensztajn,<sup>3</sup> Sandrine Florquin,<sup>2</sup> Maikel P Peppelenbosch,<sup>4</sup> C Arnold Spek<sup>1</sup>

<sup>1</sup>Center for Experimental and Molecular Medicine (CEMM) and <sup>2</sup>Department of Pathology, Academic Medical Center, University of Amsterdam, Amsterdam, the Netherlands; <sup>3</sup>Unité INSERM 700, Physiopathologie et Epidémiologie de L'Insuffisance Respiratoire, Faculté de Médecine Xavier Bichat, Paris, France; and <sup>4</sup>Department of Gastroenterology and Hepatology, Erasmus Medical Center, Rotterdam, the Netherlands

Accumulating evidence shows that protease-activated receptor-1 (PAR-1) plays an important role in the development of fibrosis, including lung fibrosis. However, whether PAR-1 also plays a role in the development of skin fibrosis remains elusive. The aim of this study was to determine the role of PAR-1 in the development of skin fibrosis. To explore possible mechanisms by which PAR-1 could play a role, human dermal fibroblasts and keratinocytes were stimulated with specific PAR-1 agonists or antagonists. To investigate the role of PAR-1 in skin fibrosis, we subjected wild-type and PAR-1-deficient mice to a model of bleomycin-induced skin fibrosis. PAR-1 activation leads to increased proliferation and extra cellular matrix (ECM) production, but not migration of human dermal fibroblasts (HDF) *in vitro*. Moreover, transforming growth factor (TGF)- $\beta$  production was increased in keratinocytes upon PAR-1 activation, but not in HDF. The loss of PAR-1 *in vivo* significantly attenuated bleomycin-induced skin fibrosis. The bleomycin-induced increase in dermal thickness and ECM production was reduced significantly in PAR-1-deficient mice compared with wild-type mice. Moreover, TGF- $\beta$  expression and the number of proliferating fibroblasts were reduced in PAR-1-deficient mice although the difference did not reach statistical significance. This study demonstrates that PAR-1 contributes to the development of skin fibrosis and we suggest that PAR-1 potentiates the fibrotic response mainly by inducing fibroblast proliferation and ECM production.

Online address: <http://www.molmed.org>

doi: 10.2119/molmed.2014.00027

## INTRODUCTION

Skin fibrosis is a devastating pathology that occurs during different human pathologies, that is, systemic sclerosis (SSc), an autoimmune disease of unknown etiology characterized by progressive fibrosis of the skin and internal organs (1), or wound-associated skin repair (2). Injury of the skin can ultimately lead to scar formation, like keloid and hypertrophic scars (3). Although the clinical appearance of the different skin disorders might differ, the activation, prolif-

eration and migration of resident fibroblasts at the site of trauma which induces deposition of extracellular matrix (ECM) proteins like fibronectin and collagen is a common pathway in these disorders (3–5). Targeting fibroblast activation and/or function may thus provide new therapeutic strategies in the treatment of fibroproliferative skin disorders due to its direct antifibrotic effect (4).

Protease activated receptor (PAR)-1 is a G-coupled receptor belonging to the protease activated receptor family that

consists of 4 members (PAR-1 to PAR-4). PARs show a unique mechanism of activation, being proteolytically cleaved by serine proteases (6). Removal of the N-terminal extracellular domain releases a tethered ligand that binds to the body of the receptor to induce transmembrane signaling (7). Interestingly, PAR-1 induces proliferation, migration and ECM production of fibroblasts and PAR-1 deficiency (either genetic or pharmacologic) limits experimental fibrosis in lung (8,9) and liver (10). In the skin, PAR-1 is expressed on keratinocytes, endothelial cells and fibroblasts and the density of PAR-1 positive fibroblasts is increased in the skin of SSc patients compared with that of healthy controls (11). Moreover, PAR-1 is expressed in both the epidermis and dermis of normal and hypertrophic scars and in keloid lesions (12). The functional consequence of PAR-1 expression in the skin remains elusive however although accelerated wound healing in

**Address correspondence to** JanWillem Duitman, Center for Experimental and Molecular Medicine, Academic Medical Center, Meibergdreef 9, NL-1105 AZ Amsterdam, the Netherlands. Phone: +31 20 56 66 034; Fax: +31 20 69 77 192; E-mail: [J.W.Duitman@amc.uva.nl](mailto:J.W.Duitman@amc.uva.nl).

Submitted February 11, 2014; Accepted for publication May 14, 2014; Epub (www.molmed.org) ahead of print May 15, 2014.

The Feinstein Institute  
for Medical Research 

Empowering Imagination. Pioneering Discovery.®

mice after topical PAR-1 activation pinpoints PAR-1 as an important receptor in the skin (13).

Here we show that PAR-1 drives profibrotic responses of human dermal fibroblasts (HDF) and keratinocytes *in vitro*. Furthermore, we show that PAR-1 plays a pivotal role in the development of skin fibrosis in a murine model of bleomycin-induced skin fibrosis.

## MATERIALS AND METHODS

### Animals

Heterozygous PAR-1-deficient mice on a C57Bl/6 background were purchased from The Jackson Laboratory (Bar Harbor, ME, USA) (14). Animals were intercrossed to obtain homozygous PAR-1 knockout (KO) mice as described before (15). Wild-type C57BL/6 mice were purchased from Charles River (Maastricht, the Netherlands). All experiments were approved by the Institutional Animal Care and Use Committee of the University of Amsterdam. All mice were maintained according to institutional guidelines. Animal procedures were carried out in compliance with the Institutional Standards for Humane Care and Use of Laboratory Animals of the Academic Medical Center. The Animal Care and Use Committee of the Academic Medical Center approved all experiments.

### Induction of Skin Fibrosis

Eight- to ten-wk-old male mice ( $n = 8$  per group) received daily intradermal injections of bleomycin (100  $\mu\text{L}$  containing 10  $\mu\text{g}$  bleomycin sulphate in PBS) into their shaved backs for 10 consecutive days.

### Histological Analysis of Skin

After euthanization, skin sections were fixed in formalin, embedded in paraffin and 4- $\mu\text{m}$ -thick sections were subsequently deparaffinized, rehydrated and washed in deionized water. Slides were stained with hematoxylin and eosin (H&E) and Masson trichrome according to routine procedures. Dermal thickness

was measured on H&E stained slides using pictures taken at 10 $\times$  magnification. The average of three measurements per section was used for each skin section.

### In Vivo Proliferation

Proliferative cells were detected using a rabbit anti-Ki67 (#RM-9106; Thermo Fisher Scientific Inc., Waltham, MA, USA) antibody essentially as described before (16). In short, after deparaffinization and endogenous peroxidase inhibition, sections were boiled in citrate buffer (pH 6.0) for 10 min, blocked with normal goat serum for 30 min and incubated overnight with the primary antibody (1:500) at 4°C. Subsequently, slides were incubated with Brightvision PolyHRP-anti-rabbit IgG (DPVR-110HRP; Immunologic, Duiven, the Netherlands) for 30 min at room temperature and stained using DAB (BS04-999; Immunologic). Per section, proliferating cells of the dermis were counted excluding cells of the epidermis, hair follicles and sebaceous glands from the analysis. Control experiments leaving out the primary antibody were performed as controls to exclude nonspecific binding of the secondary antibody.

### ECM Immunohistochemistry

Collagen type I staining was performed essentially as described before (17). For fibronectin stainings, sections were boiled in citrate buffer (pH 6.0) for 20 min, blocked with 5% normal rabbit serum in PBS for 30 min and incubated overnight with the primary antibody (1:50; sc-6953, Santa Cruz Biotechnology Inc., Dallas, TX, USA) at 4°C. Subsequently, slides were incubated with a rabbit-anti-goat-HRP antibody (1:100; P0160, Dako Netherlands B.V., Heverlee, Belgium) for 30 min at room temperature and stained using DAB (BS04-999; Immunologic). Control experiments leaving out the primary antibody were performed as controls to exclude nonspecific binding of the secondary antibody. The percentage of ECM-positive area per high power field (expressing the density of ECM) and per skin section (indicating

total amount of ECM in the dermis) was determined with ImageJ software (U.S. National Institutes of Health, Bethesda, MD, USA; <http://rsb.info.nih.gov/ij>, 1997–2011).

### Cell Culture

Human keratinocytes (HaCaT cells) (a gift from Henri H Versteeg; passages 50–55) and human dermal fibroblasts (HDFs) (American Type Culture Collection [ATCC], Manassas, VA, USA; passages 2–6) were maintained in Dulbecco's modified eagle medium (DMEM) supplemented with 10% fetal calf serum (FCS). Unless stated otherwise, cells were serum-starved for 4 h and subsequently stimulated as described. Cells were lysed in Laemmli lysis buffer, incubated for 5 min at 95°C and stored at –20°C for further analysis. Medium of the cells was stored at –20°C for TGF- $\beta$  detection.

### Lentiviral Knockdown of PAR-1

For lentiviral PAR-1 silencing, PAR-1 and control shRNA in the pLKO.1-puro backbone were purchased from Sigma-Aldrich (St. Louis, MO, USA) (MISSION shRNA library). We selected clones TRCN0000003689 (CCGGCCCCGT CATTCTCTCAGGACTCGAGTCCT GAGAAGAAATGACCGGGTTTTT), TRCN0000003691 (CCGGCCTACT ACTTCTCAGCCTTCTCTCGAGAGAA GGCTGAGAAGTAGTAGGTTTTT) and SHC003 (CCGGCGTGATCTTCACCGAC AAGATCTCGAGATCTTGTCGGTGAA GATCACGTTTTT; control; shTGF $\beta$ ). Lentiviral production and cell transduction was performed using standard protocols (18) and shRNA transduced HDFs were selected in the presence of 2  $\mu\text{g}/\text{mL}$  puromycin for 72 h.

### Cell Viability Assays

HDFs, seeded in 96-well plates at a concentration of 5000 cells/well, were stimulated with thrombin (1 U/mL), PAR-1 agonist peptide (H-SFLLRN-NH<sub>2</sub>; PAR-1-AP; 100  $\mu\text{mol}/\text{L}$ ) or human recombinant TGF- $\beta$  (5 ng/mL) after which cell viability was determined using a 3-(4,5-dimethylthiazol-2-yl)-2,5-diphenyltetrazolium (MTT) assay

according to routine procedures. When indicated, cells were preincubated for 30 min with P1pal-12 (palmitate-RCLSSAVANRS-NH<sub>2</sub>; 5  $\mu$ mol/L).

### Western Blot

Samples were subjected to sodium dodecyl sulfate/polyacrylamide gel electrophoresis (SDS-PAGE) (10% gel), after which proteins were transferred onto Immobilon-P membranes (Merck Millipore, Billerica, MA, USA) as described before (19). Next, membranes were blocked for 1 h at room temperature either in Odyssey Blocking buffer (OBB) (LI-COR Biosciences, Lincoln, NE, USA) mixed with phosphate buffered saline (PBS) in a 1:1 (vol/vol) ratio for p44/42 or in 5% bovine serum albumin in Tris-buffered saline + 0.1% Tween-20 (TBS-T) for fibronectin, collagen type I and  $\alpha$ -tubulin. The membranes were incubated overnight at 4°C with antibodies against fibronectin (1:1000 in TBS-T; sc-6953, Santa Cruz Biotechnology),  $\alpha$ -tubulin (1:1000 in TBS-T; sc-23948, Santa Cruz Biotechnology), collagen type I (1:800 in TBS-T; #1310-01, Southern Biotech, Birmingham, AL, USA) or phospho-p44/42 (1:1000 in OBB/PBS [1:1 {vol/vol} ratio]; #9106, Cell Signaling Technology, Danvers, MA, USA). After washing, the blots were incubated with secondary antibodies (HRP-conjugated for fibronectin, collagen type I and  $\alpha$ -tubulin (1:1000 in TBS-T) or IRDye 700-GAR for phospho-p44/42 (1:5000 in OBB/PBS [1:1 {vol/vol} ratio] with 0.04% SDS). Finally, membranes were imaged using Lumi-Light (12015200001; Roche, Basel, Switzerland) on an ImageQuant LAS 4000 biomolecular imager (GE Healthcare, Zeist, the Netherlands) or on a LI-COR Odyssey IR Imager.

### TGF- $\beta$ Detection

Active TGF- $\beta$  levels were measured by enzyme-linked immunosorbent assay (ELISA) (R&D Systems Inc., Minneapolis, MN, USA) according to the manufacturer's recommendations. For *in vitro* experiments, total TGF- $\beta$  levels were determined. Before start of the assay, samples

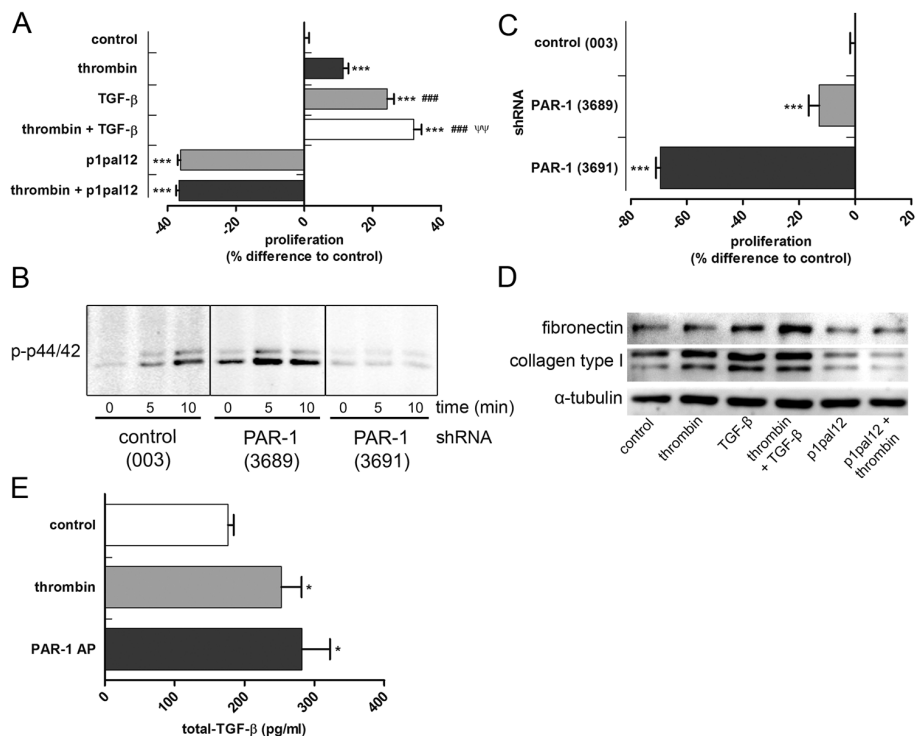


**Figure 1.** PAR-1 activation increases proliferation and ECM production in HDF and TGF- $\beta$  production in HaCaT cells. (A) MIT assay of HDFs stimulated for 24 h with thrombin (1 U/mL), TGF- $\beta$  (5 ng/mL) or the combination of both with or without pretreated for 30 min with p1pal-12 (5  $\mu$ mol/L) or saline. (B) Western blot analysis of phospho-p44/42 in cell lysates of PAR-1 (or control) shRNA transduced HDF stimulated with PAR-1-AP (100  $\mu$ mol/L) for 5 or 10 min. (C) MIT assay of control shRNA or PAR-1 shRNA transduced HDF cultured for 24 h under normal culture conditions. (D) Western blot analysis of fibronectin, collagen type I and  $\alpha$ -tubulin in HDF stimulated for 24 h with thrombin (1 U/mL), p1pal-12 (5  $\mu$ mol/L) and TGF- $\beta$  (5 ng/mL) or combinations thereof. (E) Total TGF- $\beta$  production of HaCaT cells upon PAR-1 activation with thrombin (1 U/mL) or PAR-1-AP (100  $\mu$ mol/L). Figures are representative of three independent experiments performed with  $n = 3-8$ . Data are means  $\pm$  SEM. \* $p < 0.05$  to control, \*\*\* $p < 0.001$  to control, ### $p < 0.001$  to thrombin stimulation,  $\Psi\Psi p < 0.01$  to TGF- $\beta$  stimulation.

were incubated with 1 N HCl to cleave all pro-TGF- $\beta$  and subsequently with 1.2 N NaOH/0.5 mol/L HEPES to neutralize the reaction.

### Statistical Analysis

For the *in vivo* experiment, differences between groups were analyzed by two-tailed *t* test or two-tailed Mann-Whitney *U* test for nonparametric values. For the *in vitro* experiments, 1-way analysis of variance (ANOVA) analysis or Kruksal-Wallis test (for nonparametric values) was performed, followed by the Bonferroni and Dunn multiple comparison tests, respectively. Analyses were per-

formed using GraphPad Prism version 4.0 (GraphPad Software, San Diego, CA, USA).

### RESULTS

#### PAR-1 Induces Fibrotic Responses in Keratinocytes and Dermal Fibroblasts

To assess whether PAR-1 drives fibrotic responses *in vitro*, HDFs were cultured in the presence or absence of thrombin and/or TGF- $\beta$  (positive control). As shown in Figure 1A, both thrombin-dependent PAR-1 activation and TGF- $\beta$  stimulation increased proliferation of HDFs, whereas the combina-

tion of thrombin and TGF- $\beta$  further increased proliferation. Thrombin did not induce proliferation in the presence of a specific PAR-1 antagonist (that is, P1pal-12) showing that thrombin indeed acts via PAR-1 (see Figure 1A). Interestingly, PAR-1 inhibition not only prevented thrombin-induced proliferation of HDFs but actually significantly decreased HDF proliferation, even in the absence of endogenous thrombin. Overall, these data suggest that HDF proliferation is PAR-1 dependent.

Although P1pal-12 is used frequently as a specific PAR-1 inhibitor (8) and no toxicity has been described, we next aimed to confirm that PAR-1 drives HDF proliferation. To this end, HDFs were lentivirally transduced with two different PAR-1 shRNA constructs (designated 3689 and 3691) and a control shRNA construct (003). As shown in Figure 1B, PAR-1 activation by PAR-1-AP rapidly induces phosphorylation of the well-known PAR-1 target p44/42 in shRNA 003-transduced cells. Importantly, PAR-1 signaling was effectively reduced in HDFs transduced with shRNA 3691 as evident from the absence of p44/42 phosphorylation upon stimulation with PAR-1-AP. shRNA 3689 was less effective in reducing PAR-1 signaling as evident from residual p44/42 phosphorylation after PAR-1 activation.

As expected, effective inhibition of PAR-1 signaling (that is, shRNA 3691) significantly inhibited HDF proliferation (even more effective than observed for P1pal-12 treatment), whereas noneffective PAR-1 inhibition (that is, shRNA 3689) only showed a 15% reduction in proliferation as compared with control HDFs (Figure 1C). Taken together, these data show that HDF proliferate (in part) in a PAR-1-dependent manner. As opposed to proliferation, PAR-1 stimulation did not influence HDF migration (data not shown).

Next we assessed whether PAR-1 would modify ECM production by HDFs. Indeed, thrombin stimulation of HDFs slightly increased the production of collagen type I, but it did not modify

fibronectin levels (Figure 1D). PAR-1 inhibition by P1pal-12 pretreatment abolished thrombin-induced collagen production but also diminished baseline collagen levels, showing that PAR-1 induces ECM synthesis. As expected, TGF- $\beta$  stimulation also induced collagen and fibronectin production. Interestingly, the combination of thrombin and TGF- $\beta$  further induced fibronectin levels without significantly affecting collagen levels.

PAR-1 deficiency reduces TGF- $\beta$  levels during pulmonary fibrosis (9) and TGF- $\beta$  is important in the pathogenesis of skin fibrosis (20). Consequently, we wondered whether PAR-1 could also potentiate skin fibrosis by inducing TGF- $\beta$  production. As shown in Figure 1E, both thrombin and PAR-1-AP stimulation of HaCaT cells indeed induced TGF- $\beta$  production (as measured by total TGF- $\beta$  production in the supernatant of the cells). In contrast, TGF- $\beta$  levels produced by HDFs were low and did not change upon PAR-1 activation (data not shown). Overall, these data suggest that PAR-1 plays an important role during dermal fibrosis by modifying HDF proliferation and ECM production and potentially by enhancing TGF- $\beta$  production by keratinocytes.

### Reduction of Bleomycin-Induced Skin Fibrosis by Loss of PAR-1

To determine whether PAR-1 is critical for skin fibrosis, we subjected PAR-1-deficient and wild-type mice to a bleomycin-induced skin fibrosis model. As shown in Figures 2A–C, dermal thickness was increased significantly due to bleomycin treatment and this increase was significantly diminished in PAR-1-deficient mice as compared with wild-type mice. In line, the accumulation of ECM also was reduced in PAR-1-deficient mice as compared to wild-type mice, as evident from reduced collagen content in Masson trichrome-stained skin sections (Figure 2D). To discriminate between different collagen types, we next performed specific immunohistochemical stainings for collagen type I and III. Interestingly, the density of collagen type I did not differ between bleomycin-treated

wild-type and PAR-1-deficient mice (Figures 2E, F), whereas the total amount of collagen type I was increased in the dermis of wild-type versus PAR-1-deficient mice (Figures 2E, G). Collagen type III expression was rather low in both wild-type and PAR-1-deficient mice (data not shown). Together, these data show that PAR-1 deficiency limits bleomycin-induced skin fibrosis.

### Modification of Profibrotic Responses in PAR-1-deficient mice

In our *in vitro* experiments (Figure 1), we showed that PAR-1 drives fibroblast proliferation and, consequently, we next determined the number of proliferating cells in the dermis of bleomycin-treated wild-type and PAR-1-deficient mice. As shown in Figures 3A and B, the number of proliferating cells, as analyzed by the number of Ki67 positive cells per skin section, was reduced in PAR-1-deficient mice as compared to wild-type mice, although the difference did not reach statistical significance. As already indicated, TGF- $\beta$  production by keratinocytes was induced by PAR-1 activation *in vitro*, and TGF- $\beta$  is important in the pathogenesis of skin fibrosis (20). As shown in Figure 3C, however, active TGF- $\beta$  levels were not significantly different in skin homogenates of wild-type and PAR-1-deficient mice upon bleomycin treatment. Finally, we determined fibronectin expression in the skin of wild-type and PAR-1-deficient animals and, in line with our *in vitro* experiments, fibronectin levels per skin section were reduced in PAR-1-deficient mice as compared with wild-type mice (Figures 3D, F) whereas the density of fibronectin did not differ between bleomycin-treated wild-type and PAR-1-deficient mice (Figures 3D, E).

### DISCUSSION

PAR-1 plays an important role during the initiation and progression of both lung and liver fibrosis (8–10). Here, we determined whether PAR-1 also would drive skin fibrosis. Indeed, PAR-1 activation leads to increased proliferation and



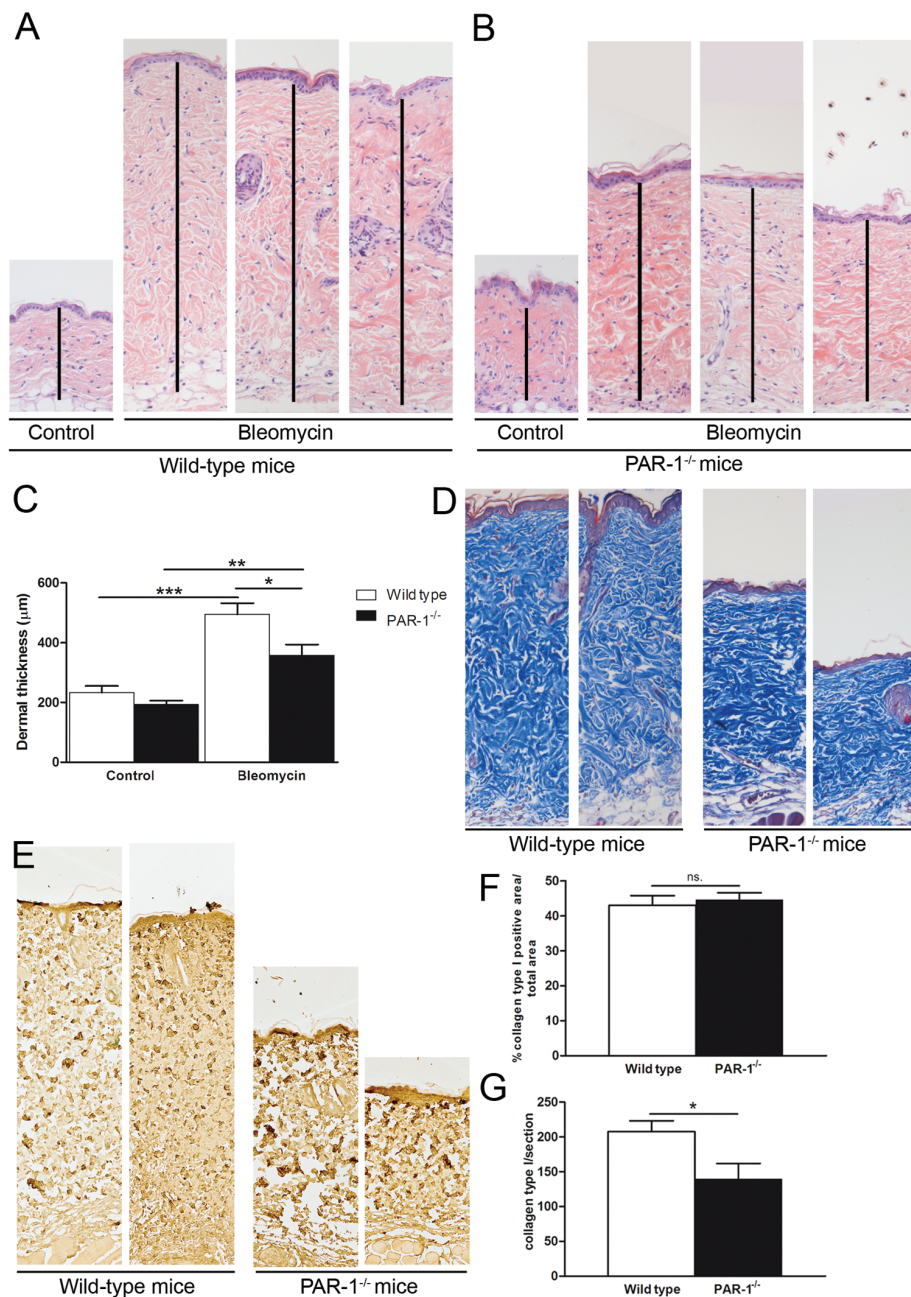


**Figure 2.** PAR-1 contributes to skin fibrosis in a model of bleomycin-induced skin fibrosis. (A–B) H&E staining of skin sections of wild-type (A) and PAR-1-deficient (B) mice upon bleomycin treatment (10× magnification). The dermis is indicated with a black vertical line. (C) Quantification of the dermal thickness upon bleomycin treatment in wild-type and PAR-1-deficient mice (n = 7–8). (D) Representative pictures of Masson trichrome staining of skin sections from wild-type and PAR-1-deficient mice upon bleomycin treatment (10× magnification). (E) Representative pictures of collagen type I expression in skin sections from wild-type and PAR-1-deficient mice upon bleomycin treatment (10× magnification). (F) Density of collagen type I in the dermis of bleomycin-treated wild-type and PAR-1-deficient mice. (G) Total amount of collagen type I per dermal section of bleomycin-treated wild-type and PAR-1-deficient mice. Data are means ± SEM. \**p* < 0.05, \*\**p* < 0.01 and \*\*\**p* < 0.001. n.s., Not significant.

ECM production in HDFs, whereas it also potentiates TGF-β production of keratinocytes. In line with these *in vitro* data, we also show reductions in dermal thickening and collagen/fibronectin deposition in PAR-1-deficient mice during experimental skin fibrosis. Overall, our data thus pinpoint PAR-1 as a novel mediator of skin fibrosis.

Our *in vitro* data suggest that PAR-1 modifies skin fibrosis by acting as a pleiotropic mediator affecting multiple profibrotic responses (that is, proliferation, TGF-β production and ECM deposition). However, during experimental skin fibrosis, PAR-1 deficiency only showed significant effects on ECM deposition, whereas the differences in fibroblast proliferation did not reach statistical significance. It may thus be that PAR-1 mainly affects ECM deposition during bleomycin-induced skin fibrosis, although the observed variability in fibroblast proliferation *in vivo* may explain the lack of significance. TGF-β production also was not significantly reduced in PAR-1-deficient mice, which may be due to the fact that PAR-1 only contributes to TGF-β production in keratinocytes and not in dermal fibroblasts. As PAR-1 modifies inflammation during pulmonary fibrosis (9), it may be tempting to speculate that PAR-1-dependent inflammation may potentiate skin fibrosis. Importantly however, inflammatory cell influx (neutrophils and macrophages) and cytokine production were similar in bleomycin-treated wild-type and PAR-1-deficient mice (data not shown).

An interesting finding of our manuscript is the fact that PAR-1 inhibition (both pharmacologically and genetically) reduces proliferation and ECM production of HDFs. These data strongly suggest that HDFs secrete an endogenous PAR-1 agonist that drives proliferation and ECM production under normal culture conditions in an autocrine manner. Expression levels of the endogenous PAR-1 ligand seem to be rate limiting for these profibrotic processes as exogenous PAR-1 activation still further increases both proliferation and ECM production.

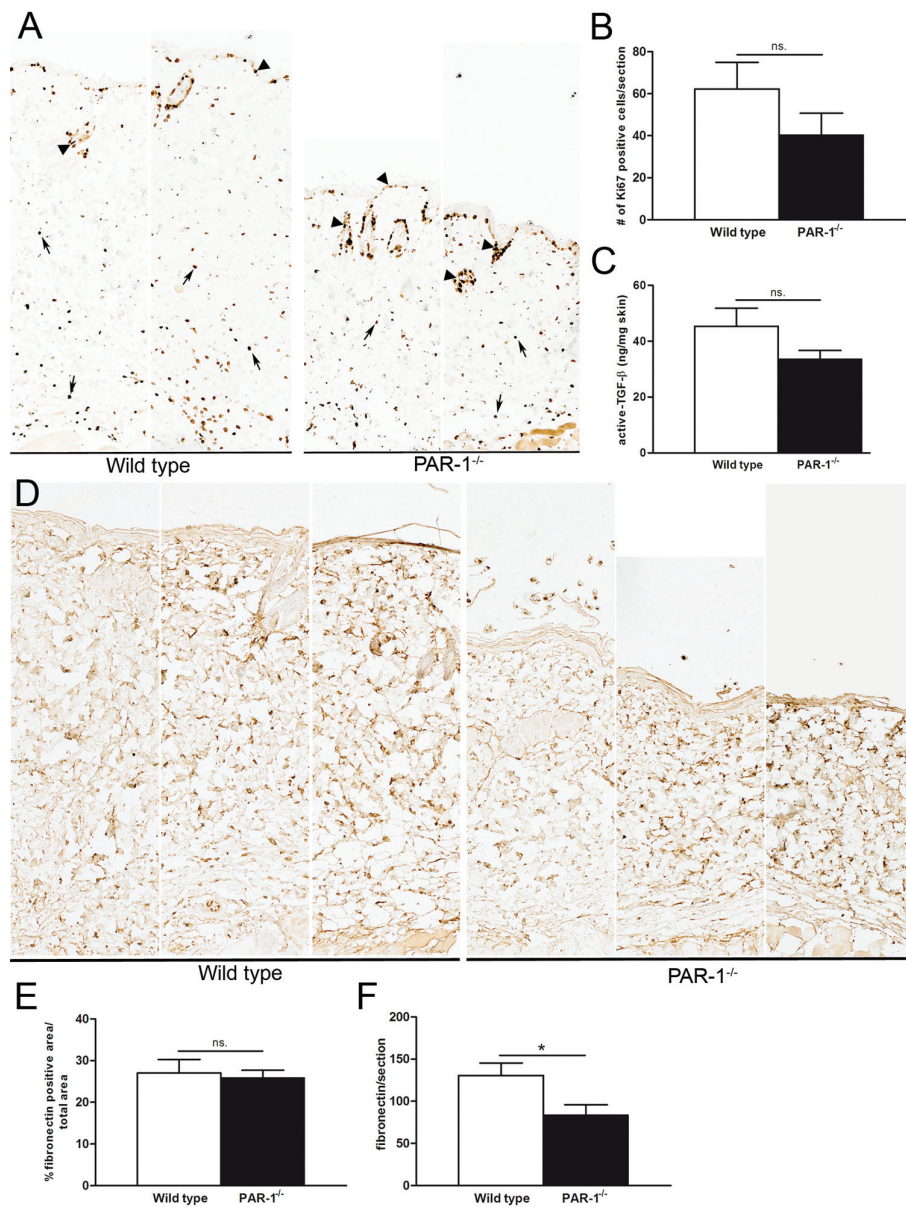


**Figure 3.** Modification of profibrotic processes by PAR-1 *in vivo*. (A) Immunohistochemical staining of Ki67-positive cells in skin sections of wild-type and PAR-1-deficient mice upon bleomycin treatment (10× magnification). (B) Quantification of Ki67 positive cells in the dermis (excluding cells of hair follicles and sebaceous glands (arrow heads in panel A)) of wild-type and PAR-1-deficient mice upon bleomycin treatment ( $n = 4-7$ ). (C) Active TGF- $\beta$  levels in skin homogenates of wild-type and PAR-1-deficient mice upon bleomycin treatment ( $n = 7-8$ ). (D) Representative pictures of fibronectin expression in skin sections from wild-type and PAR-1-deficient mice upon bleomycin treatment (10× magnification). (E) Density of fibronectin in the dermis of bleomycin-treated wild-type and PAR-1-deficient mice ( $n = 5-6$ ). (F) Total amount of fibronectin per dermal section of bleomycin-treated wild-type and PAR-1-deficient mice. Data are means  $\pm$  SEM. \* $p < 0.05$ . n.s., Not significant.

Although several PAR-1 agonists (such as MMP13 [21] and kallikreins [22]) have been described to be produced in skin fi-

broblasts, the exact nature of the endogenous PAR-1 agonist remains elusive and is currently under investigation.

We used a bleomycin-induced model of skin fibrosis that largely mimics human scleroderma (23). Indeed, dermal thickening is accompanied by deposition of dense packed collagen fibrils that are extensively cross linked in both murine and human scleroderma. The fact that we show that PAR-1 deficiency limits skin fibrosis in this model, together with the fact that PAR-1 expression is increased in the skin during human Ssc (11) and that PAR-1 activation on human cell types potentiates key profibrotic processes, suggests that PAR-1 may have clinical relevance for human scleroderma. Besides increased PAR-1 expression in scleroderma, PAR-1 also is expressed in other skin disorders such as normal and hypertrophic scars and keloid lesions (12), and PAR-1 might, consequently, also play a role in the development of these disorders. Before targeting PAR-1 in patients, one should realize, however, that PAR-1 also mediates platelet activation and targeting PAR-1 could lead to bleeding complications. It may consequently be better to target the still elusive endogenous PAR-1 agonist.

## CONCLUSION

In conclusion, we identify PAR-1 as a novel potential mediator of skin fibrosis which may open novel therapeutic treatment strategies for limiting skin fibrosis (or other cutaneous fibrotic disorders) for which no effective treatment strategies are available at this time.

## ACKNOWLEDGMENTS

This study was supported by Grant 09.102 from the Dutch Burns Foundation to J Duitman. The authors like to thank Marieke ten Brink and Joost Daalhuisen for their technical assistance during the animal experiments.

## DISCLOSURE

The authors declare that they have no competing interests as defined by *Molecular Medicine*, or other interests that might be perceived to influence the results and discussion reported in this paper.



## REFERENCES

1. Gabrielli A, Svegliati S, Moroncini G, Amico D. (2012) New insights into the role of oxidative stress in scleroderma fibrosis. *Open Rheumatol. J.* 6:87–95.
2. Shaw TJ, Kishi K, Mori R. (2010) Wound-associated skin fibrosis: mechanisms and treatments based on modulating the inflammatory response. *Endocr. Metab. Immune Disord. Drug Targets.* 10:320–30.
3. Canady J, Karrer S, Fleck M, Bosserhoff AK. (2013) Fibrosing connective tissue disorders of the skin: Molecular similarities and distinctions. *J. Dermatol. Sci.* 70:151–8.
4. Gilbane AJ, Denton CP, Holmes AM. (2013) Scleroderma pathogenesis: a pivotal role for fibroblasts as effector cells. *Arthritis Res. Ther.* 15:215–23.
5. Leask A, Abraham DJ. (2004) TGF-beta signaling and the fibrotic response. *FASEB J.* 18:816–27.
6. Vu TKH, Hung DT, Wheaton VI, Coughlin SR. (1991) Molecular-cloning of a functional thrombin receptor reveals a novel proteolytic mechanism of receptor activation. *Cell.* 64:1057–68.
7. Ramachandran R, Hollenberg M. (2008) Proteinases and signalling: pathophysiological and therapeutic implications via PARs and more. *Br. J. Pharmacol.* 153:S263–82.
8. Lin C, et al. (2014) Targeting protease activated receptor-1 with P1pal-12 limits bleomycin-induced pulmonary fibrosis. *Thorax.* 69:152–60.
9. Howell DCJ, et al. (2005) Absence of proteinase-activated receptor-1 signaling affords protection from bleomycin-induced lung inflammation and fibrosis. *Am. J. Pathol.* 166:1353–65.
10. Rullier A, et al. (2008) Protease-activated receptor 1 knockout reduces experimentally induced liver fibrosis. *Am. J. Physiol. Gastrointest. Liver Physiol.* 294:G226–35.
11. Cevikbas F, et al. (2011) Role of protease-activated receptors in human skin fibrosis and scleroderma. *Exp. Dermatol.* 20:69–71.
12. Materazzi S, et al. (2007) Analysis of protease-activated receptor-1 and-2 in human scar formation. *J. Pathol.* 212:440–9.
13. Strukova SM, et al. (2001) Immobilized thrombin receptor agonist peptide accelerates wound healing in mice. *Clin. Appl. Thromb. Hemost.* 7:325–9.
14. Connolly AJ, Ishihara H, Kahn ML, Farese RV, Coughlin SR. (1996) Role of the thrombin receptor in development and evidence for a second receptor. *Nature.* 381:516–9.
15. Schouten M, van't Veer C, Roelofs JJ, Levi M, van der Poll T. (2012) Protease-activated receptor-1 impairs host defense in murine pneumococcal pneumonia: a controlled laboratory study. *Crit. Care.* 16:R238.
16. Bijlsma MF, et al. (2008) Endogenous hedgehog expression contributes to myocardial ischemia-reperfusion-induced injury. *Exp. Biol. Med. (Maywood).* 233:989–96.
17. Duitman J, et al. (2014) CCAAT-enhancer binding protein delta (C/EBPdelta) attenuates tubular injury and tubulointerstitial fibrogenesis during chronic obstructive nephropathy. *Lab. Invest.* 94:89–97.
18. Anastasov N, et al. (2009) Efficient shRNA delivery into B and T lymphoma cells using lentiviral vector-mediated transfer. *J. Hematop.* 2:9–19.
19. Duitman J, et al. (2012) CCAAT/enhancer-binding protein delta facilitates bacterial dissemination during pneumococcal pneumonia in a platelet-activating factor receptor-dependent manner. *Proc. Natl. Acad. Sci. U. S. A.* 109:9113–8.
20. Yamamoto T, Takagawa S, Katayama I, Nishioka E. (1999) Anti-sclerotic effect of transforming growth factor-beta antibody in a mouse model of bleomycin-induced scleroderma. *Clin. Immunol.* 92:6–13.
21. Ravanti L, et al. (2001) Expression of human collagenase-3 (MMP-13) by fetal skin fibroblasts is induced by transforming growth factor-beta via p38 mitogen-activated protein kinase. *FASEB J.* 15:1098–100.
22. Komatsu N, et al. (2003) Expression and localization of tissue kallikrein mRNAs in human epidermis and appendages. *J. Invest. Dermatol.* 121:542–9.
23. Vorstenbosch J, et al. (2013) CD109 overexpression ameliorates skin fibrosis in a mouse model of bleomycin-induced scleroderma. *Arthritis Rheum.* 65:1378–83.